

Atom Counting in Expanding Ultracold Clouds

Sibylle Braungardt¹, Mirta Rodríguez², Aditi Sen(De)³, Ujjwal Sen³, and Maciej Lewenstein^{1,4}

¹*ICFO-Institut de Ciències Fotòniques, Mediterranean Technology Park, 08860 Castelldefels (Barcelona), Spain*

²*Instituto de Estructura de la Materia, CSIC, Serrano 121, 28006 Madrid, Spain*

³*Harish-Chandra Research Institute, Chhatnag Road, Jhansi, Allahabad 211 019, India*

⁴*ICREA - Institució Catalana de Recerca i Estudis Avançats,
Passeig Lluís Companys 23, E-08010 Barcelona, Spain*

We study the counting statistics of ultracold bosonic atoms that are released from an optical lattice. We show that the counting probability distribution of the atoms collected at a detector located far away from the optical lattice can be used as a method to infer the properties of the initially trapped states. We consider initial superfluid and insulating states with different occupation patterns. We analyze how the correlations between the initially trapped modes that develop during the expansion in the gravitational field are reflected in the counting distribution. We find that for detectors that are large compared to the size of the expanded wave function, the long-range correlations of the initial states can be distinguished by observing the counting statistics. We consider counting at one detector, as well as the joint probability distribution of counting particles at two detectors. We show that using detectors that are small compared to the size of the expanded wave function, insulating states with different occupation patterns, as well as supersolid states with different density distributions can be distinguished.

I. INTRODUCTION

Experiments with ultracold particles trapped in optical lattices aim towards the engineering of exotic many-body quantum states [1]. Recently, the trapping and cooling of dipolar gases have attracted much attention [2]. The dipole moments induce long-range interactions between the particles, and new phases appear [3]. In the strongly correlated regime, it has been shown that there are many quasi degenerate metastable insulating states with defined occupation patterns [4–7]. These metastable states could be used for the storage and processing of quantum information in analogy to classical neural networks, where the information is robustly encoded in the distributed stable states of a complex system [8, 9]. Another way to induce long-range interactions between atoms trapped in an optical lattice is via coupling to an external cavity mode. This has just recently been achieved experimentally and a checkerboard to a supersolid transition has been observed [10].

The detection of exotic strongly correlated phases requires novel experimental techniques that give access to high-order correlation functions. Proposals for detection techniques typically make use of shot-noise measurements [11] or atom-light interfaces [12]. Also, the counting statistics of atoms has been suggested as a technique able to distinguish strongly correlated [13, 14] and fermionic [15] Hamiltonians, both at zero and finite temperature [16]. The detection of single atoms trapped in the optical lattice has become experimentally available [17–20] only recently. Most counting experiments are performed after switching off the trapping potential and letting the atoms propagate in the gravitational field. The counting statistics of Rb atoms falling within a high-finesse cavity has been reported in Ref. [21]. Also, fermionic and bosonic counting probability distributions have been measured for metastable Helium atoms falling

onto a microchannel plate [22, 23].

The theoretical analysis of the counting process has so far mainly been considered for atoms trapped in the lattice. Propagation in the gravitational field mixes the initial modes of the atoms, such that the counting statistics in the lattice and after propagation are not expected to be the same. In this paper, we study the role of expansion in the counting process. We show that the mixing of the initial modes during the expansion becomes evident in the counting distribution when the detector is small compared to the size of the expanded wave function. We illustrate the effect by analyzing the counting statistics for bosons after time-of-flight expansion from the lattice. We consider initial states with different occupation patterns in the insulating regime and supersolid states with different density distributions in the superfluid regime. We calculate both the counting probabilities at a single detector and the joint probabilities at two detectors as a function of the horizontal distance between them. We show that a superfluid (SF) and Mott insulator (MI) state can be readily distinguished by their counting statistics. We further show that a suitable choice of the detector geometry allows for the detection of different occupation patterns in the insulating regime and different supersolid states.

The paper is organized as follows. In Sec. II we review the propagation of the atomic wave functions and the atom counting formalism. In Sec. III we analyze the intensity of particles arriving at the detector, which consists of auto-correlation terms and crossed-correlations between the different expanded modes. Depending on the size and geometry of the detector, the ratio between the auto-correlations and the crossed-correlation terms changes. In Sec. IV we obtain closed expressions for the counting distributions for expanded superfluid and insulating bosonic states. We consider the counting statistics when using one detector and the joint counting distribu-

tion at two detectors. In Sec. V, we show our results and compare the SF with MI states and insulating states with different occupation patterns.

II. DESCRIPTION OF THE SYSTEM

We consider neutral bosonic atoms trapped in an optical lattice. The system can be described using the Bose-Hubbard model [24], which includes the hopping of the particles between neighbouring sites and the on-site two-body interactions. At zero temperature, the two limiting cases of the phase diagram are the SF state, where the hopping term dominates, and the MI state, where local interactions are dominant. The field operator $\Psi(\mathbf{r}, t)$ of the many-body system can be expanded into the N modes a_i

$$\Psi(\mathbf{r}, t) = \sum_i \phi_i(\mathbf{r}, t) a_i. \quad (1)$$

For atoms trapped in an optical lattice, a_i describes the destruction of a particle on site i . The corresponding initial wave functions are Wannier functions which are Gaussian functions centered at \mathbf{r}_i

$$\phi_i(\mathbf{r}, t=0) = \frac{1}{(\pi\omega^2)^{3/4}} e^{-(\mathbf{r}-\mathbf{r}_i)^2/2\omega^2}, \quad (2)$$

where the width ω is chosen such that the initial wave functions at different sites i do not overlap.

The atoms are released from the optical lattice and expand in the gravitational field. At finite t , we can apply the single-particle expansion

$$\phi(\mathbf{r}, t) = \int d\mathbf{r}' K(\mathbf{r}, \mathbf{r}', t) \phi_i(\mathbf{r}', 0) \quad (3)$$

where the propagator for the free expansion in the gravitational field reads [25]

$$K(\mathbf{r}, \mathbf{r}', t) = \left(\frac{m}{2\pi i \hbar t} \right)^{3/2} e^{\frac{im(\mathbf{r}-\mathbf{r}')^2}{2\hbar t} - \frac{imgt(z+z')}{2\hbar} - \frac{im^2 g^2 t^3}{24m\hbar}}. \quad (4)$$

The full propagated wave function is then written as

$$\phi_i(\mathbf{r}, t) = \frac{e^{-\frac{im^2 g^2 t^3}{24m\hbar}}}{\pi^{3/4} (i\omega_t + \omega)^{3/2}} e^{-\frac{(\mathbf{r}-\mathbf{r}_i)^2}{2(\omega_t^2 + \omega^2)}} e^{-i\frac{(\mathbf{r}-\mathbf{r}_i)^2 \omega_t}{2\omega(\omega_t^2 + \omega^2)}}, \quad (5)$$

where and $\mathbf{r}_t = \mathbf{r} + \mathbf{z}_t$, with $\mathbf{z}_t = (0, 0, gt^2/2)$ and we have used that $|\mathbf{r}_t - \mathbf{r}_i| \gg \omega$. Note that in the limit of $\omega_t \gg \omega$, the expanded wave function is, up to a phase factor, a Gaussian function centered around \mathbf{z}_t with a width $\omega_t = \hbar t / (m\omega)$.

A. Atom counting

We describe a counting process in which the probability $p(m)$ of counting m particles within a time interval τ

is measured at a detector located at a distance z_0 from the lattice. The probability of detecting m particles can be expressed as [26, 27]

$$p(m) = \frac{(-1)^m}{m!} \frac{d^m}{d\lambda^m} \mathcal{Q} \Big|_{\lambda=1}, \quad (6)$$

where the generating function $\mathcal{Q}(\lambda)$ is given by the expectation value of a normally ordered exponential of the intensity \mathcal{I} ,

$$\mathcal{Q}(\lambda) = \text{Tr}(\rho : e^{-\lambda \mathcal{I}} :). \quad (7)$$

For photons, the intensity is proportional to an integral over the product of the negative-frequency part and the positive-frequency part of the field. The normal ordering $: \dots :$ reflects the detection mechanism, in which the photons are absorbed at the detector, typically a photo multiplier or an avalanche photodiode. For the detection of atoms using microchannel plates, the detection process can be treated in an analogous way.

Since typically not all the particles are counted, the intensity depends on the efficiency ϵ of the detector and the detection time τ . When the dynamics of the measurement are fast in comparison to the dynamics of the system, the intensity is proportional to the factor $\kappa \equiv 1 - e^{-\epsilon\tau}$. For typical experimental situations, the dynamics of the system are determined by the expansion of the atomic cloud in the gravitational field, given by ω_t and the intensity can be described by the integral over the detector volume Ω of the positive-frequency and negative-frequency parts of the quantum fields describing the particles to be counted, multiplied by the efficiency factor κ [28],

$$\mathcal{I} = \kappa \int_{\Omega} d\mathbf{r} \Psi^\dagger(\mathbf{r}, t_d) \Psi(\mathbf{r}, t_d), \quad (8)$$

where t_d denotes the time at which the instantaneous measurement is performed.

The formalism described above is easily generalized to the case of detection with multiple detectors [29]. For detection with M detectors, the generating function reads

$$\mathcal{Q}_M(\lambda_1, \lambda_2, \dots, \lambda_M) = \text{Tr}(\rho : e^{-\sum_i \lambda_i \mathcal{I}_i} :), \quad (9)$$

where the single detector intensity \mathcal{I}_i for each of the detectors is given by eq. (8). For a configuration with two detectors, the joint probability distribution of counting m atoms at detector 1 and n atoms at detector 2 is given by

$$p(m, n) = \frac{(-1)^{m+n}}{m!n!} \frac{d^{m+n}}{d\lambda_1^m d\lambda_2^n} \mathcal{Q}_2 \Big|_{\lambda_1=1, \lambda_2=1}. \quad (10)$$

We study the correlations $\text{corr}(m, n)$ between the counting events detected at each detector by observing the ratio between the covariance and the single detector variances,

$$\text{corr}(m, n) = \frac{\text{cov}(m, n)}{\sigma^2(m)\sigma^2(n)}, \quad (11)$$

where $\text{cov}(m, n) = \sum_{m, n} mnp(m, n) - \bar{m}\bar{n}$, \bar{m} denotes the mean and $\sigma^2(m)$ the variance of $p(m)$.

III. DETECTION OF EXPANDING ATOMS

Let us now discuss the counting process for the detection of atoms expanding in the gravitational field. We consider a cubic detector located at a distance z_0 from the lattice center with edge lengths $\Delta_x, \Delta_y, \Delta_z$. For simplicity, all through this paper we consider $t_d = \sqrt{2z_0/g}$ which is the time when the center of the cloud arrives at the detector. The intensity \mathcal{I} of atoms registered at the detector defined in eq. (8) is thus determined by the expanded field operator of the atoms at the time t_d of detection, $\Psi(z_0, t_d)$. Using eqs. (1) and (8), the intensity \mathcal{I} takes the form

$$\mathcal{I} = \sum_{ij} A_{ij} a_i^\dagger a_j, \quad (12)$$

where

$$A_{ij}(z_0, \Omega, \kappa) = \kappa \int_{\Omega} d\mathbf{r} \phi_i^*(z_0, t_d) \phi_j(z_0, t_d). \quad (13)$$

The elements of the correlation matrix A_{ij} defined in eq. (13) describe the interference and autocorrelation terms between different modes registered at the detector. The diagonal terms represent the on-site correlations, whereas the off-diagonal terms represent the crossed-correlations between single particle modes initially located at different sites with distance $|i - j|$.

Before studying the full counting distribution, let us consider the correlations given by the matrix elements A_{ij} . Using eq. (5) and assuming $\omega_{t_d} \gg \omega$, the autocorrelation elements are given by

$$A_{ii} = \kappa \int_{\Omega} d\mathbf{r} \frac{1}{\pi^{3/2} \omega_{t_d}^3} e^{-\frac{(\mathbf{r}-\mathbf{r}_i)^2}{\omega_{t_d}^2}}. \quad (14)$$

For expanded wave functions at $\mathbf{r} \gg \mathbf{r}_i$, the autocorrelations become all equal and independent of the original lattice site i . The crossed-correlations are given by

$$A_{ij} = \kappa \int_{\Omega} d\mathbf{r} \frac{1}{\pi^{3/2} \omega_{t_d}^3} e^{-\frac{(\mathbf{r}-\mathbf{r}_i)^2}{\omega_{t_d}^2}} e^{-i\frac{\mathbf{r}(\mathbf{r}_i-\mathbf{r}_j)}{\omega \omega_{t_d}}} \quad (15)$$

The ratio between the crossed correlations and the autocorrelations depend crucially on the geometry of the detector.

In Fig. 1, we show the on-site correlations eq. (14) and the interference terms eq. (15) in function of the size of the detector. We consider a one dimensional array in z -direction and plot the correlations at the location of the detector at $(0, 0, z_0)$. We consider a fixed detector size in the x - y -plane, $\Delta = \Delta_x = \Delta_y$ and vary its width Δ_z . Depending on the size of the detector, the whole cloud or a fraction of it is registered. For $z_0 = 1$ cm, the size of the expanded single-particle wave function at the detector is $\omega_{t_d} = 0.8$ mm. In Fig. 1 a, we show that for detectors of size $\Delta_z > 0.2$ mm, the interference terms are negligible. This is easily understood from eq.

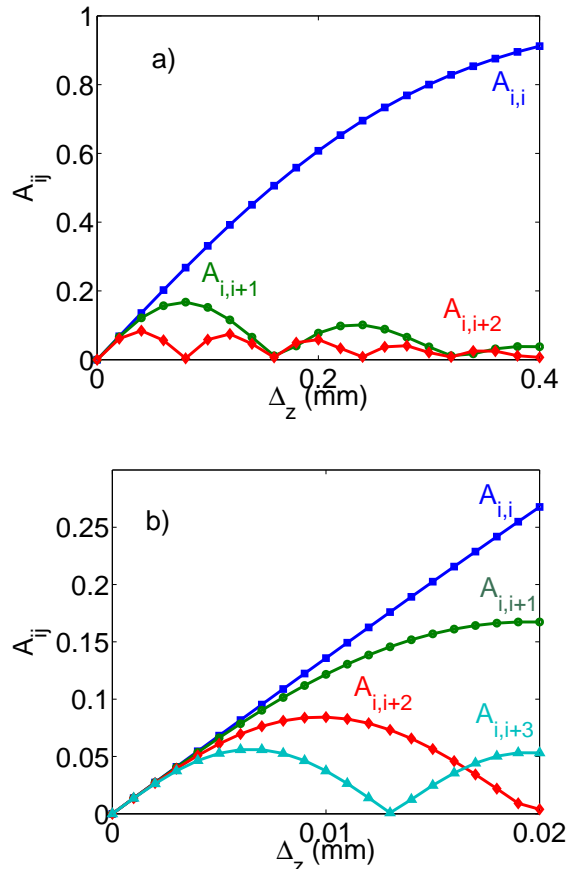


FIG. 1: The ratio between the on-site-correlations and interference terms depend on the size of the detector. a) Wide detector limit $\Delta_z \simeq \omega_t$. b) Narrow detector limit $\Delta_z \ll \omega_t$. We plot A_{ii} (blue squares) $A_{i,i+1}$ (green circles), $A_{i,i+2}$ (red diamonds), and $A_{i,i+3}$ (light blue triangles). Parameters used: $z_0 = 1$ cm, $\Delta_x = \Delta_y = 1$ cm and $\kappa = 1$

(14), as the auto-correlations are given by an integral over the detector volume around the center of a Gaussian function. For detectors that are large compared to the size of the cloud, the on-site correlations approach unity. In contrast, the interference terms eq. (15) are given by the integral over a Gaussian function multiplied by a highly oscillating phase, such that they approach zero as the size of the detector increases. Thus, for on-site counting and for detectors which are larger than the size of the cloud, the crossed correlations disappear $A_{ij} \simeq 0$ for $i \neq j$, while the auto-correlations approach $A_{ii} \simeq \kappa$.

As we show below, the detection of the auto-correlations between different modes is sufficient to distinguish the long-range correlations in the system. In particular, we show that a MI state can be distinguished from a SF.

On the contrary, as the auto-correlation terms for different sites are equal, distinguishing states with different occupation patterns cannot be achieved in this limit. Fig. 1 b shows that for small detector sizes, the interference

terms are of the order of the on-site correlations. We will show that in this limit, different occupation patterns are distinguishable from the counting distribution.

IV. ATOM COUNTING STATISTICS

Let us now consider the counting distributions measured at the detector after the expansion for different initial states of the system of atoms trapped in the lattice.

A. Superfluid state

First, let us focus on a SF state, ground state of the Bose-Hubbard model for very shallow lattices. We derive the counting distribution using the Gutzwiller ansatz [30] for the wave function which assumes that it is a product of on-site coherent states. The initial state of the atoms in the lattice with N sites then reads:

$$|\psi\rangle = \prod_i^N |\alpha_i\rangle_i, \quad (16)$$

where $|\alpha_i\rangle_i$ is the coherent state on site i ,

$$|\alpha_i\rangle_i = e^{-|\alpha_i|^2/2} \sum_{n=0}^{\infty} \frac{\alpha_i^n}{\sqrt{n!}} |n\rangle_i \quad (17)$$

and $|n\rangle_i = (a_i)^n |0\rangle$ is a Fock state with n particles. Note that $|\psi\rangle$ is an eigenstate of the annihilation operator $\Psi(\mathbf{r}, t)$ of the expanded atoms,

$$\Psi(\mathbf{r}, t)|\psi\rangle = \sum_i \phi_i(\mathbf{r}, t) \alpha_i |\psi\rangle, \quad (18)$$

where ϕ_i is given by eq. (2). The state $|\psi\rangle$ is thus an eigenstate of the expanded field operator $\Psi(\mathbf{r}, t)$ and we can write the generating function as $\mathcal{Q}(\lambda) = e^{-\lambda \sum_{ij} \alpha_i^* \alpha_j A_{ij}}$. Using eq. (6) the counting distribution $p(m)$ reads

$$p(m) = \frac{\left(\sum_{ij} \alpha_i^* \alpha_j A_{ij}\right)^m}{m!} e^{-\sum_{ij} \alpha_i^* \alpha_j A_{ij}}, \quad (19)$$

where A_{ij} is given by eq. (13).

For a homogeneous superfluid with equal mean number of particles per sites, $\alpha_i = \alpha$ for all i , and in the limit of big detectors where the diagonal elements of the matrix A_{ij} are much bigger than the off-diagonal elements, the counting distribution of the SF simplifies to

$$p(m) = \frac{(N|\alpha|^2 A_d)^m}{m!} e^{-N|\alpha|^2 A_d}, \quad (20)$$

which corresponds to a Poissonian distribution with mean (and thus also variance) $\bar{m} = \sigma^2(m) = |\alpha|^2 A_d$.

B. Mott Insulator state

Let us now consider the Mott insulating regime. We first study a Mott insulator state with one particle per site, $|\psi\rangle = |11\dots 11\rangle$. In this case, the generating function eq. (7) reads

$$\begin{aligned} \mathcal{Q}(\lambda) &= \langle 11\dots 11 | : e^{-\lambda \kappa \int_{\Omega} d\mathbf{r} \Psi^\dagger(\mathbf{r}, t_d) \Psi(\mathbf{r}, t_d)} : | 11\dots 11 \rangle \\ &= 1 - \lambda \sum_i A_{ii} + \lambda^2 \sum_{i < j} (A_{ii} A_{jj} + |A_{ij}|^2) - \dots \end{aligned} \quad (21)$$

We can rewrite eq. (21) using the minors of the matrix A ,

$$\mathcal{Q}(\lambda) = 1 + \sum_{k=1}^N (-1)^k \lambda^k M_+(A, k), \quad (22)$$

where $M_+(A, m)$ denotes the permanent $\text{perm}(A) = \sum_{\sigma \in S_n} \prod_{i=1}^n A_{i, \sigma(i)}$ of the corner blocks of size m of the matrix A . Note that $M_+(A, k)$ is closely related to the principal minors of the matrix, which are defined as the determinant of the respective block matrices. The counting distribution $p(m)$ can then be calculated using Eqs. (6) and (22).

As was outlined above, in typical experimental situations the detector is far away from the lattice and much bigger than the cloud, such that the off-diagonal elements of A_{ij} are negligible and the diagonal elements A_{ii} are equal for all i . In this case the generating function \mathcal{Q} for the Mott insulator state with unit filling is given by

$$\mathcal{Q}(\lambda) = \sum_{k=0}^N \binom{N}{k} (-\lambda A_d)^k = (1 - A_d \lambda)^N, \quad (23)$$

where A_d denotes any of the (equal) diagonal elements. The counting distribution $p(m)$ is then given by

$$p(m) = \binom{N}{m} A_d^m (1 - A_d)^{N-m} \quad (24)$$

This corresponds to the distribution of a fock state. The mean \bar{m} and variance $\sigma^2(m)$ of the distribution are given by

$$\bar{m} = N A_d, \quad \sigma^2(m) = N A_d (1 - A_d) \quad (25)$$

Let us now consider the different occupation patterns that arise in the strongly correlated regime. In particular, we focus on such states where at most one particle occupies each site. The generating function is then calculated by eq. (22), with a correlation matrix A' , composed of the elements of the correlation matrix A in eq. (13) multiplied by the occupation numbers n_i and n_j of the involved sites,

$$A' = n_i n_j A_{ij}. \quad (26)$$

Finally, let us consider a symmetric superposition of all possible states with filling factor N_p/N_s , where N_p is

the number of particles, N_s denotes the number of sites and $N_p \leq N_s$, the generating function reads

$$\mathcal{Q} = 1 + \sum_m (-1)^m \lambda^m \mathcal{F}_{MI}(A, m, N_p, N_s), \quad (27)$$

where

$$\begin{aligned} \mathcal{F}_{MI}(A, m, N_p, N_s) &= \frac{\binom{N_s-m}{N_p-m}}{\binom{N_s}{N_p}} M^+(A, m) \\ &+ \frac{\binom{N_s-2m}{N_p-m}}{\binom{N_s}{N_p}} 2^m \mathcal{K}(m), \end{aligned} \quad (28)$$

where $\mathcal{K}(m)$ is defined as the m fold product over the sum with non-repeated indices of the real part of A_{ij} , $\sum_{i<j} \text{Re}(A_{ij})$. For $m=2$, e.g. $M_+ = \sum_{i<j} (A_{ii}A_{jj} + |A_{ij}|^2)$ and $\mathcal{K}(m) = \text{Re}(A_{ij})\text{Re}(A_{kl})$ with $k, l \neq i, j$.

C. Counting at two detectors

In this section, we consider the detection of the MI and SF state using two detectors and study the correlations between the counting events.

For the MI state, the joint counting distribution $p(m, n)$ of counting m particles at one detector and n particles at the other is given by eq. (10), where the generating function for two detectors is given by

$$\mathcal{Q}_2 = \sum_{k=1}^N (-1)^k M^+(\lambda_1 A^{(1)} + \lambda_2 A^{(2)}, k). \quad (29)$$

For detectors that are located symmetrically with respect to the origin in the x - y -plane, in typical experimental situations the off-diagonal elements of A_{ij} are negligible (see fig. 1), and the diagonal elements A_d are all equal for both detectors, $A_d^{(1)} = A_d^{(2)} = A_d$. The generating function thus simplifies to

$$\begin{aligned} \mathcal{Q}_2(\lambda_1, \lambda_2) &= \sum_{k=0}^N \binom{N}{k} (-A_d)^k (\lambda_1 + \lambda_2)^k \\ &= (1 - A_d(\lambda_1 + \lambda_2))^N, \end{aligned} \quad (30)$$

and the counting distribution is given by

$$\begin{aligned} p(m, n) &= (-1)^{n+m} (1 - 2A_d)^{Np-m-n} \times \\ &(-A_d)^{m+n} \frac{Np!}{m!n!(Np-m-n)!} \end{aligned} \quad (31)$$

For the SF state, the joint counting distribution $p_{SF}(m, n)$ is the product of the two single detector distributions $p_1(m)$ and $p_2(n)$ given by eq. (19). The counting events at the two detectors are thus not correlated.

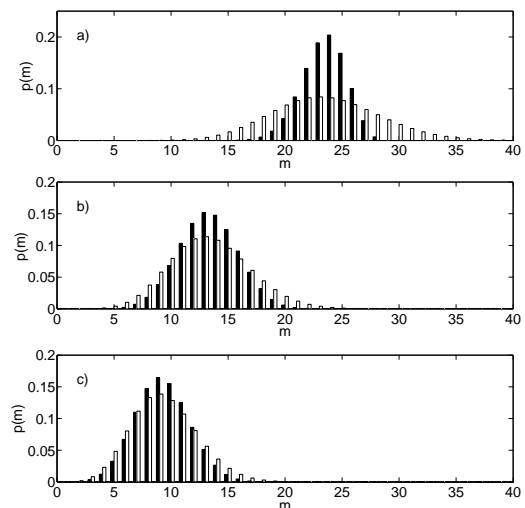


FIG. 2: MI vs. SF as a function of distance from detector. Probability distribution for MI (black bars) and superfluid (white bars) states in a $3 \times 3 \times 3$ lattice. $\Delta_x = \Delta_y = 2$ mm, $\Delta_z = 2$ cm, $\kappa = 1$. a) $z_0 = 1$ cm, b) $z_0 = 3$ cm, c) $z_0 = 5$ cm

V. RESULTS

A. Mott Insulator and Superfluid state

We consider the counting distributions of a SF and a MI state of bosons with the same average number of particles released from a three dimensional optical lattice. We assume the limit of a large detector, where the counting distribution is determined by the on-site correlation terms. In Fig. 2, we plot the counting distributions for a SF and a MI state at different distances between the detector and the lattice. With increasing distance from the detector, a smaller fraction of the expanded wave function is registered. The difference between the MI and the SF becomes less visible, and the mean of the counting distribution decreases. In Fig. 3, we plot the mean and the variance of the counting distributions, both normalized by dividing by N , for the superfluid and the Mott insulator state for a detector with fixed size at different distances z_0 from the lattice.

B. Mott Insulator and Superfluid state with two detectors

Let us now consider two detectors of the same size that are placed symmetrically at a distance $\mathbf{x}_1 = (x_d, 0, z_0)$ and $\mathbf{x}_2 = (-x_d, 0, z_0)$ from the lattice center. In the limit of large detectors, we study the joint counting distribution of the SF and MI state for different distances between the detectors. Fig. 4 shows the counting distributions for two overlapping detectors (left column) and for two detectors separated by $2x_d = 1$ cm (right column). For the SF state, shown in the lower row in figs.

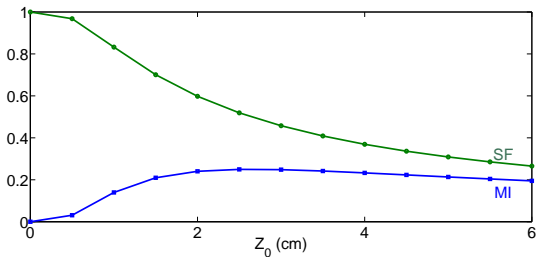


FIG. 3: $\sigma^2(m)/N$ of the counting distribution for the MI (blue squares) and SF (green circles) state with respect to the distance from the detector z_0 . $\Delta_x = \Delta_y = 2$ mm, $\Delta_z = 2$ cm, $\kappa = 1$.

4, the joint counting distribution is a Gaussian function for both cases. This is expected, as the joint counting distribution eq. (19) is a product of the single detector counting distributions. This is analogous to the detection of coherent states of light. For the MI state shown in the upper row in fig. 4, we observe a squeezed distribution, indicating the correlations of the atoms counted at the two detectors. Note that as the distance between the detectors increases, the squeezing of the distribution is less pronounced. The correlations between the counting events at the two detectors can be seen more clearly when looking at the correlation function eq. (11). Note that for the superfluid state, there is no difference between the joint counting distribution and the product of the single particle distributions. For the Mott state, we study the correlations for varying distance between the two detectors x_d . In Fig. 5, we show how the correlations decrease when increasing the distance between detectors x_d . Note that the distance x_d denotes the distance between the center of the two detectors. For $x_d = 0$, the detectors fully overlap, and for $x_d > \Delta$ the detectors are completely separated.

C. Detection of insulating states with different occupation patterns

Let us now focus on the detection of insulating states with different occupation patterns by particle counting. As discussed above, in order to detect the different patterns, the crossed-correlations have to be of the order of the autocorrelations. This is clear as away from the lattice, all the on-site correlation terms become equal. Let us discuss the example of a checkerboard state, where every second site is occupied, and a state with stripes, where every second line is occupied. For the striped state, the leading crossed-correlation terms eq. (15) are the ones that correspond to the nearest neighbors. For the checkerboard state, where neighboring sites are not occupied, the leading terms are the ones that correspond to diagonally adjacent sites. In order to distinguish the different patterns, it is thus essential that these two leading crossed-terms are sufficiently different and at the same

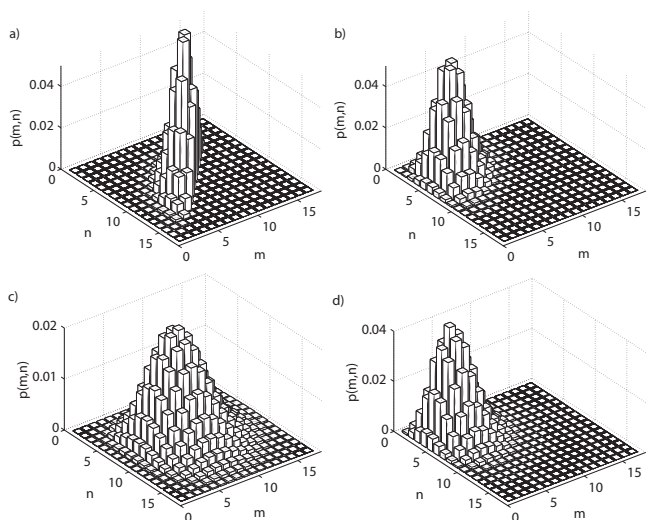


FIG. 4: Joint probability distribution of an expanded MI (upper row) and a SF (lower row) in a 4×4 lattice with two symmetrically placed detectors. In fig. a) and c) $x_d = 0$. In fig. b) and d) $x_d = 1$ cm. Parameters used: $z_0 = 1$ cm, $\Delta_z = 2$ mm, $\Delta_x = \Delta_y = 2$ cm, $\kappa = 0.5$.

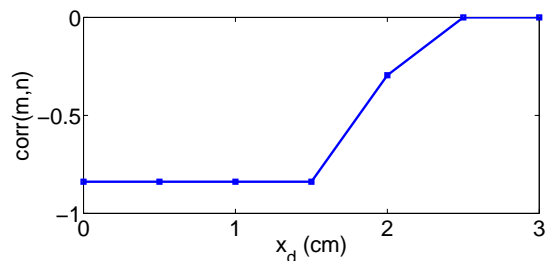


FIG. 5: Correlations of the joint probability distribution for an expanded MI state with two symmetrically placed detectors. As the distance between the detectors increases, the counting events at the two detectors are no longer correlated. Parameters used: $z_0 = 1$ cm, $\Delta_z = 2$ mm, $\Delta_x = \Delta_y = 2$ cm, $\kappa = 0.5$

time comparable to the on-site correlations. From Fig. 1, we see that this implies that the limit of small detectors has to be considered. However, if the detector is very small, all the terms are equal and the patterns are not distinguishable. One should thus consider an intermediate detector size.

In Fig. 6, we illustrate the effect for a 1D system of $N = 12$ particles. We compare the counting distributions of a checkerboard-like state, where every second site is occupied, and a state where a block of six sites is occupied and a block of six sites is empty. In order to distinguish the two states, from Fig. 1, we choose a detector size of $\Delta = 0.02$ mm, such that the ratio of the crossed-correlation terms between neighboring sites and the autocorrelations is 0.6. Fig. 6 shows that the different occupation patterns are reflected in the counting distribution.

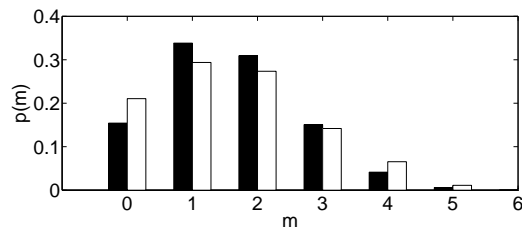


FIG. 6: The counting distributions of an expanded one-dimensional checkerboard (black bars) and striped insulating pattern (white bars) are clearly distinguishable. Parameters used: $z_0 = 1$ cm, $\Delta = 0.1$ cm, $\Delta_z = 0.02$ mm, $\kappa = 1$, $N_p = 12$

D. Detection of a Supersolid state

As for the detection of states with different occupation patterns in the insulating regime, the detection of supersolid states [31, 32] requires the limit where the crossed-correlation terms for neighboring sites are comparable to the auto-correlation terms. We consider a supersolid state with N sites and mean density $\alpha_{2i} = \beta$ and $\alpha_{2i-1} = \gamma$. For the limit where the crossed-correlation terms for neighboring sites are the only non-negligible interference terms, the counting distribution eq. (19) is given by a Poissonian distribution with mean

$$\bar{m} = \frac{N}{2} A_d (\beta^2 + \gamma^2) + 2N A_{NN} \beta \gamma, \quad (32)$$

where A_d denotes the diagonal elements corresponding to the on-site correlations and A_{NN} denotes the nearest neighbor crossed-correlation terms. Let us compare this to a superfluid state with a homogeneous density per site, $|\alpha_i|^2 = \frac{|\beta|^2 + |\gamma|^2}{2}$ for all i . The counting distribution eq. (19) is thus given by a Poissonian distribution with mean

$$\bar{m} = \frac{N}{2} A_d (\beta^2 + \gamma^2) + N A_{NN} (\beta^2 + \gamma^2). \quad (33)$$

From eqs. (32) and (33) it is clear that a supersolid state can be distinguished from a superfluid state by particle counting. In Fig. 7 we illustrate this by comparing a supersolid state to a superfluid state.

VI. SUMMARY

We have studied the counting distributions of atoms falling from an optical lattice and propagating in the gravitational field. The intensity of atoms recorded at a detector located far away from an optical lattice

can be decomposed into autocorrelation and crossed-correlations between the expanding modes. The ratio between these terms depends crucially on the geometry of the detector. In the limit when the detector is large compared to the expanded modes, the crossed-correlation terms are negligible and only long-range correlations of

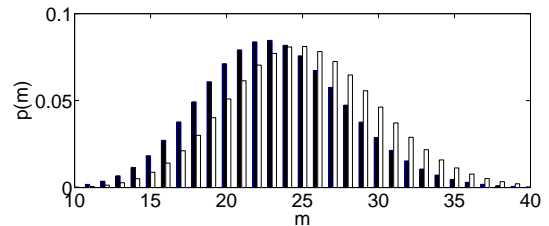


FIG. 7: The counting distributions of an expanded supersolid state with $|\beta|^2 = 0.5$ and $|\gamma|^2 = 1.5$ (black bars) and a superfluid state $|\alpha|^2 = 1$ (white bars) are clearly distinguishable. Parameters used: $z_0 = 1$ cm, $\Delta = 1$ cm, $\Delta_z = 0.02$ mm, $\kappa = 1$

different states can be distinguished. In this limit a SF state has a poissonian number distribution while a MI has subpoissonian number distribution for a detector of finite size located at a distance z_0 from the lattice. The two states can also be readily distinguished from the joint probability distribution of counting the particles at two detectors. In the SF regime, the joint probability distribution is a product of the two independent number distributions while in the MI regime, the distributions are highly correlated.

When the detector is small compared to the expanded wave function, the crossed-correlation terms for adjacent sites are of the order of the auto-correlations. We have shown that by choosing the size of the detector in an appropriate way, different occupation patterns can be distinguished by particle counting after expansion both in the insulating as well as in the superfluid regime.

Acknowledgments

We acknowledge financial support from the Spanish MICINN project FIS2008-00784 (TOQATA), FIS2010-18799, Consolider Ingenio 2010 QOIT, EU-IP Project AQUTE, EU STREP project NAMEQUAM, ERC Advanced Grant QUAGATUA, the Ministry of Education of the Generalitat de Catalunya, and from the Humboldt Foundation. M.R. is grateful to the MICINN of Spain for a Ramón y Cajal grant, M.L. acknowledges the Alexander von Humboldt Foundation and Hamburg Theoretical Physics Prize.

[1] M. Lewenstein, A. Sanpera, V. Ahufinger, B. Damski, A. Sen(De), and U. Sen, *Adv. Phys.* **56**, 243 (2007).

[2] T. Lahaye, C. Menotti, L. Santos, M. Lewenstein, and T. Pfau, *Rep. Prog. Phys.* **72**, 126401 (2009).

- [3] G. G. Batrouni and R. T. Scalettar, *Phys. Rev. Lett.* **84**, 1599 (2000), P. Sengupta, L. P. Pryadko, F. Alet, M. Troyer, and G. Schmid, *Phys. Rev. Lett.* **94**, 207202 (2005), D. L. Kovrizhin, G. V. Pai, and S. Sinha, *Europhys. Lett.* **72**, 162 (2005), K. Góral, L. Santos, and M. Lewenstein, *Phys. Rev. Lett.* **88**, 170406 (2002).
- [4] C. Menotti, C. Trefzger, and M. Lewenstein, *Phys. Rev. Lett.* **98**, 235301 (2007).
- [5] C. Trefzger, C. Menotti, and M. Lewenstein, *Phys. Rev. A* **78**, 043604 (2008).
- [6] B. Capogrosso-Sansone, C. Trefzger, M. Lewenstein, P. Zoller, and G. Pupillo, *Phys. Rev. Lett.* **104**, 125301 (2010).
- [7] L. Pollet, J. D. Picon, H. P. Büchler, and M. Troyer, *Phys. Rev. Lett.* **104**, 125302 (2010).
- [8] U. Dorner, P. Fedichev, D. Jaksch, M. Lewenstein, and P. Zoller, *Phys. Rev. Lett.* **91**, 073601 (2003).
- [9] M. Pons, V. Ahufinger, C. Wunderlich, A. Sanpera, S. Braungardt, A. Sen(De), U. Sen, and M. Lewenstein, *Phys. Rev. Lett.* **98**, 023003 (2007), S. Braungardt, A. Sen(De), U. Sen, and M. Lewenstein, *Phys. Rev. A* **76**, 042307 (2007).
- [10] K. Baumann, C. Guerlin, F. Brennecke, and T. Esslinger, *Nature* **464**, 1301-1306 (2010).
- [11] E. Altman, E. Demler, and M. D. Lukin, *Phys. Rev. A* **70**, 013603 (2004).
- [12] K. Eckert, O. Romero-Isart, M. Rodríguez, M. Lewenstein, E. Polzik, and A. Sanpera, *Nature Physics* **4**, 50 (2008); D. Porras and I. Cirac, *Phys. Rev. A* **78**, 053816 (2008).
- [13] S. Braungardt, A. Sen(De), U. Sen, R. J. Glauber, and M. Lewenstein, *Phys. Rev. A* **78**, 063613 (2008).
- [14] R. W. Cherng and E. Demler, *New J. Phys.* **9**, 7 (2007).
- [15] W. Belzig, C. Schroll, and C. Bruder, *Phys. Rev. A* **75**, 063611 (2007).
- [16] S. Braungardt, M. Rodríguez, A. Sen(De), U. Sen, R. J. Glauber, and M. Lewenstein, *Phys. Rev. A* **83**, 013601 (2011).
- [17] T. Gericke, P. Würtz, D. Reitz, T. Langen, and H. Ott, *Nature Physics* **4**, 949 - 953 (2008).
- [18] N. Gemelke, X. Zhang, C.-L. Hung, and C. Chin, *Nature* **460**, 995-998 (2009).
- [19] W. S. Bakr, A. Peng, M. E. Tai, R. Ma, J. Simon, J. I. Gillen, S. Fölling, L. Pollet, and M. Greiner, *Science* **329**, 547-550 (2010).
- [20] J. F. Sherson, C. Weitenberg, M. Endres, M. Cheneau, I. Bloch, and S. Kuhr, *Nature* **467**, 68-72 (2010).
- [21] T. Stöferle, H. Moritz, C. Schori, M. Köhl, and T. Esslinger, *Phys. Rev. Lett.* **92**, 130403 (2004).
- [22] M. Schellekens, R. Hoppeler, A. Perrin, J. Viana Gomes, D. Boiron, A. Aspect, and C.I. Westbrook, *Science* **310**, 648 (2005).
- [23] T. Jeltjes, J.M. McNamara, W. Hogervorst, W. Vassen, V. Krachmalnicoff, M. Schellekens, A. Perrin, H. Chang, D. Boiron, A. Aspect, and C.I. Westbrook, *Nature* **445**, 402 (2007).
- [24] D. Jaksch, C. Bruder, J. I. Cirac, C. W. Gardiner, and P. Zoller, *Phys. Rev. Lett.* **81**, 3108 - 3111 (1998).
- [25] T. Kramer, C. Bracher, and M. Kleber, *J. Phys. A* **35**, 8361 (2002).
- [26] R.J. Glauber, in *Quantum Optics and Electronics*, eds. B. DeWitt, C. Blandin, and C. Cohen-Tannoudji, pp. 63-185 (Gordon and Breach, New York, 1965).
- [27] K.E. Cahill and R.J. Glauber, *Phys. Rev. A* **59**, 1538 (1999).
- [28] J. Grochmalicki and M. Lewenstein, *Phys. Rep.* **208**, 189 (1991).
- [29] F. T. Arecchi, A. Berné, and A. Sona, *Phys. Rev. Lett.* **17**, 260263 (1966).
- [30] W. Krauth, M. Caffarel, and J.-P. Bouchard, *Phys. Rev. B* **45**, 3137 (1992); K. Sheshadri, H. R. Krishnamurthy, R. Pandit, and T. V. Ramakrishnan, *Europhys. Lett.* **22**, 257 (1993).
- [31] A. J. Leggett, *Phys. Rev. Lett.* **25**, 1543-1546 (1970).
- [32] N. Prokof'ev, *Avd. Phys.* **56**, 381 (2007).